ORGANOMETALLICS

pubs.acs.org/Organometallics Article

Synthesis and Characterization of Tungsten Alkylidene and Alkylidyne Complexes Featuring a New Carbazole-Based Rigid Trianionic ONO^{3-} Pincer-Type Ligand

Ushnish Mandal, Sudarsan VenkatRamani, Ion Ghiviriga, Khalil A. Abboud, and Adam S. Veige*

Cite This: *Organometallics* 2020, 39, 2207−2213 Read Online

ACCESS | Metrics & More | Article Recommendations | Supporting Information

ABSTRACT: The design and synthesis of a rigid carbazole trianionic pincer ligand and its tungsten alkylidene [CBZ-ONO]W═CH^{t}Bu(O^{t}Bu) (**3**) and anionic alkylidyne {Ph_3PCH_3}{[CBZ-ONO]W≡C^{t}Bu(O^{t}Bu)} (**4**) complexes are reported. Designed to maximize the inorganic enamine effect by constraining the N atom lone pair, the carbazole ligand achieves high planarity. However, the orbital overlap remains similar to that of the flexible ligand [CF_3−ONO]H_3 (**1**). The neutral alkylidyne complex could not be synthesized. The complexes were characterized by multinuclear NMR spectroscopy, combustion analysis, mass spectrometry, and single-crystal X-ray diffraction. DFT calculations reveal an inorganic enamine orbital overlap within the alkylidyne complexes bearing both the rigid and flexible ligands.

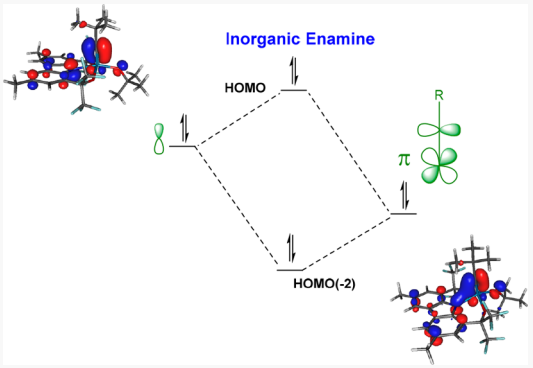

Pincer and pincer-type ligands are synthetically malleable. The donor atom combination,[1−3] charge,[4] bite angle,[5] redox activity,[6] chemical noninnocence,[7] tethering to a solid support,[8] and ligand architecture[1] are properties at the disposal of synthetic chemists for manipulating the geometric and electronic properties of metal complexes bearing pincer ligands. Among the various classes of pincer and pincer-type ligands available, trianionic pincer ligands[9] are particularly useful, as exemplified by recent applications in aerobic oxidation,[10] nitrene[11,12] and carbene transfer,[13] ethylene[14] and alkyne polymerization,[15,16] cyclic polymer synthesis,[17−21] and alkene isomerization.[22]

Pincer-type ligands where a heteroatom, in particular N, resides in the central position of the chelate offer a unique opportunity to tailor the nucleophilicity of metal−carbon multiple bonds via the inorganic enamine effect.[23] For example, the pincer-type ligand 2,2′-(azanediylbis(5-methyl-2,1-phenylene))bis(1,1,1,3,3,3-hexafluoropropan-2-ol) ([CF_3-ONO]H_3; **1**) enhances the nucleophilicity of tungsten alkylidene and tungsten alkylidyne complexes.[23] Isolobal with organic enamines, an inorganic enamine orbital interaction occurs when an amido nitrogen atom lone pair is collinear with a metal−carbon multiple bond. Figure 1 depicts a truncated molecular orbital diagram that illustrates this overlap within the {[CF_3-ONO]W≡CEt(O^{t}Bu)}$^-$ anion.[23] This orbital overlap creates a bonding and antibonding combination with the M−C π bond, and as a consequence, the HOMO orbital is destabilized, being π^* in character, and the electron density from the amido lone pair is delocalized onto the α carbon of the metal−carbon multiple bond. This dual effect leads to the

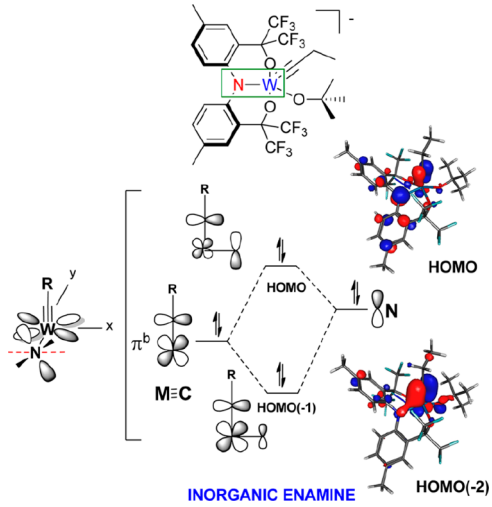

Figure 1. Inorganic enamine orbital interaction enhancement of metal−carbon multiple-bond nucleophilicity due to overlap of the amido lone pair with the tungsten alkylidyne π bonds within [CF_3-ONO]W≡CEt(O^{t}Bu)$^-$ (orbital pictures presented at isovalue 0.056187).[23] Reprinted with permission from ref 23. Copyright 2012 American Chemical Society.

Received: March 3, 2020
Published: May 1, 2020

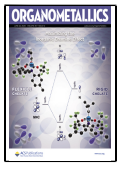

https://dx.doi.org/10.1021/acs.organomet.0c00150
Organometallics 2020, 39, 2207−2213

formation of highly nucleophilic alkylidenes and alkylidynes.[24−26] The angle of the N atom p orbital approach and its energy match with the M−C π bond naturally influences the magnitude of the orbital overlap.[27]

The trianionic pincer ligand **1** contains flanking biaryl moieties adjacent to the central amine that, when they are bound to metal ions, create an inherent twist across the pincer backbone.[23,27] Due to the twist, improper orbital alignment occurs and the inorganic enamine orbital interaction is not maximized. It is the goal of this research project to constrain the amido lone pair to be perfectly collinear with metal−carbon multiple bonds. Accomplishing this goal, we present the new rigid trianionic $[ONO]^{3-}$ C_{2v}-symmetric carbazole-based pincer ligand[28] 2,2′-(3,6-dimethyl-9*H*-carbazole-1,8-diyl)bis(1,1,1,3,3,3-hexafluoropropan-2-ol) $[CBZ\text{-}ONO]H_3$ (**2**), by linking the two aryl moieties as shown in Figure 2.

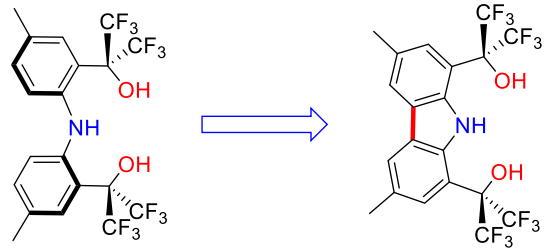

Figure 2. Approach to convert the flexible twisted biaryl pincer ligand **1** into the rigid flat pincer ligand **2**.

Preparing the ligand precursor $[CBZ\text{-}ONO]H_3$ (**2**) involves treating 1,8-dibromo-3,6-dimethyl-9*H*-carbazole[29] with 3.1 equiv of ^{n}BuLi in Et_2O and then adding hexafluoroacetone at −78 °C (Scheme 1). Warming to room temperature followed

Scheme 1. Synthesis of Proligand $[CBZ\text{-}ONO]H_3$ (2)

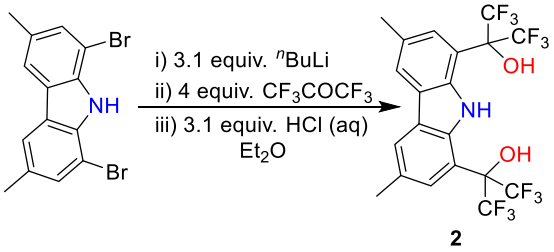

by an acidic workup and subsequent solvent evaporation yields a thick brown oil. Addition of pentane to the oil produces a solution and a black solid. Subsequent filtration and evaporation of the solvent provides a yellow solid that can be further purified to give proligand **2** in 39% yield. In the ^{19}F NMR spectrum of **2** in C_6D_6, one singlet attributable to the fluorine atoms appears at −74.77 ppm. The appearance of one signal indicates the compound is C_{2v} symmetric, implying fast rotation around the C_{aryl}−$C(CF_3)_2(OH)$ bond. Consistent with the structural assignment and symmetry, the ^{1}H NMR spectrum exhibits a singlet at 2.25 ppm for the methyl protons and two doublets at 7.66 and 7.58 ppm for the aromatic protons. Sharp resonances for both the amine and OH protons on **2** appear at 9.96 and 2.82 ppm, respectively, indicating again fast rotation on the NMR time scale. This contrasts with the previously reported flexible $[CF_3\text{-}ONO]H_3$ ligand **1**.[23] Slow rotation due to hydrogen bonding in **1** at ambient temperature led to broad NH and OH signals and two ^{19}F signals, rendering it C_2 symmetric in solution.

Treating $[CBZ\text{-}ONO]H_3$ (**2**) with $(^t\text{BuO})_3\text{W}{\equiv}\text{C}^t\text{Bu}$[30] in C_6D_6 at 50 °C yields the alkylidene complex **3** according to Scheme 2. Recrystallizing **3** in pentane provides analytically

Scheme 2. Synthesis of Tungsten Alkylidene Complex $[CBZ\text{-}ONO]W{=}CH^tBu(O^tBu)$ (3)

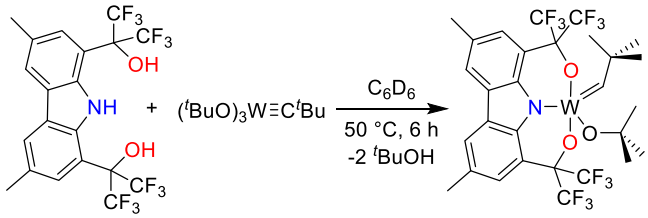

pure material in 54% yield. Single crystals amenable to X-ray diffraction deposit upon cooling a concentrated pentane solution of **3** to −35 °C. Structure refinement of the diffraction data provides the molecular structure of alkylidene **3**, depicted in Figure 3.

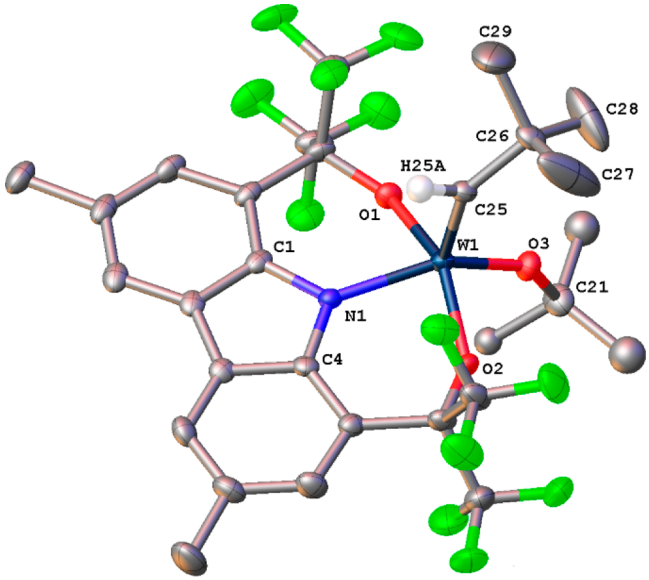

Figure 3. Molecular structure of $[CBZ\text{-}ONO]W{=}CH^tBu(O^tBu)$ (**3**) with ellipsoids drawn at the 50% probability level and hydrogen atoms removed for clarity (except H25). Selected bond distances (Å): W1−O1 1.943(1), W1−O2 1.929(3), W1−N1 2.013(4), W1=C25 1.879(5), W1−O3 1.814(3), N1−C1 1.428(6), N1−C4 1.412(6). Selected bond angles (deg): ∠O1−W1−O2 149.94(15), ∠O3−W1−N1 146.42(16), ∠W1=C25−C26 139.1(4).

Complex **3** is C_s symmetric. With a τ_5 value of 0.059,[31] the formally tungsten(VI) ion adopts a square-pyramidal geometry. The $[CBZ\text{-}ONO]^{3-}$ trianionic pincer-type ligand and the *tert*-butoxide reside on the basal plane, and the alkylidene fragment (=CH^tBu) occupies the axial position. The W=C_α bond distance of 1.879(5) Å is similar to the double-bond length of 1.882(4) Å found in the analogous complex $[CF_3\text{-}ONO]W{=}CH(Et)(O^tBu)$ (**5**), featuring the flexible pincer-type ligand.[23] As designed, the flat carbazole forces the N-aryl rings to be coplanar, making the complex C_s symmetric.

https://dx.doi.org/10.1021/acs.organomet.0c00150
Organometallics 2020, 39, 2207−2213

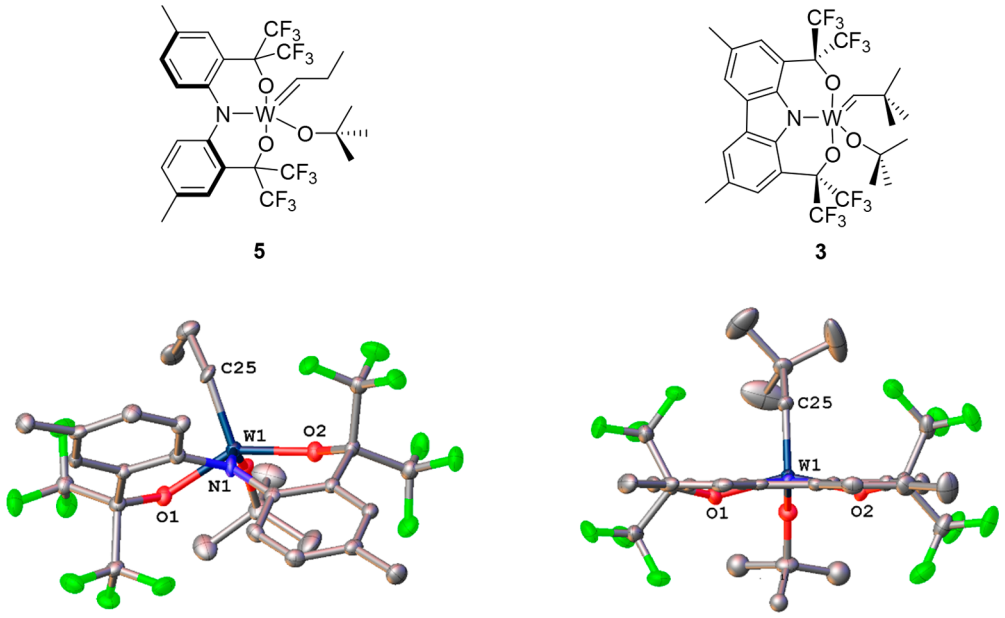

Figure 4. Comparison of the solid-state molecular structures of the flexible (**5**)[23] and rigid (**3**) trianionic pincer ligand W alkylidenes viewed along the N−W bond axis.

Consistent with the solid-state structure, the solution-phase ^{1}H NMR data exhibit resonances attributable to a C_s-symmetric complex; for example, the two Ar-CH_3 groups resonate as a singlet at 2.24 ppm.

Evidence for the alkylidene comes from a singlet signal at 6.58 ppm with satellites from coupling to ^{183}W ($^{2}J_{WH}$ = 8.80 Hz). The *tert*-butyl protons for W=CHC(CH_3)$_3$ and WOC(CH_3)$_3$ resonate at 1.12 and 1.26 ppm, respectively. Consistent with C_s symmetry, the ^{19}F NMR spectrum of **3** contains two quartets at −71.55 and −74.93 ppm. Previously characterized W alkylidenes bearing ligand **1** exhibit alkylidene carbon resonances at 260.3 and 262.6 ppm;[23,32] the corresponding signal for complex **3** similarly appears at 264.1 ppm.

Figure 4 depicts the truncated crystal structures of the W alkylidene complex **5**, featuring the flexible pincer ligand **1**,[23] and the truncated W alkylidene complex **3**, containing the new rigid ligand **2**. It is obvious that the trigonal plane comprising the N atom within complex **5** twists relative to the alkylidene W=C bond. In contrast, the trigonal plane of the N atom in complex **3** is perpendicular to the W=C bond axis.

Treating a pentane solution of **3** with Ph_3PCH_2[33,34] deprotonates the alkylidene and precipitates the anionic alkylidyne complex {[CBZ-ONO]W≡C^{t}Bu(O^{t}Bu)}-{CH_3PPh_3} (**4**) as a yellow powder in 80% yield (Scheme 3). The NMR data support the assignment of complex **4** as a C_s-symmetric anionic alkylidyne. The ^{1}H NMR spectrum of **4** (C_6D_6) contains a doublet at 1.92 ppm corresponding to the $PPh_3CH_3^+$ countercation, and the ^{31}P{^{1}H} NMR spectrum contains a single resonance at 20.38 ppm. The downfield resonance at 288.7 ppm in the ^{13}C{^{1}H} NMR spectrum of **4** provides strong support for its assignment as an alkylidyne. Four other reported [ONO]$^{3-}$ trianionic pincer ligand supported anionic W alkylidyne α carbons resonate at 280.6, 286.0, 290.6, and 301.1 ppm.[23,32,35−37] In addition, a single methyl resonance at 2.48 ppm in the ^{1}H NMR spectrum and two quartets at −70.62 and −75.47 ppm in the ^{19}F NMR spectrum are consistent with the C_s-symmetric structural assignment.

Scheme 3. Synthesis of Anionic Tungsten Alkylidyne Complex [CBZ-ONO]W≡C^{t}Bu(O^{t}Bu) (4)

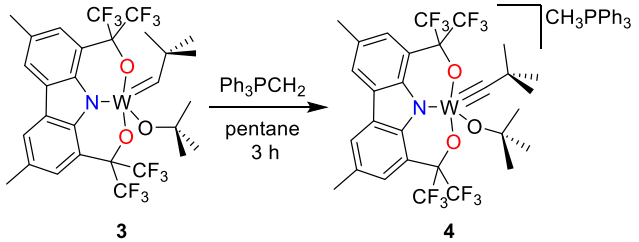

Unfortunately, converting the anionic alkylidyne complex **4** to its neutral derivative [CBZ-ONO]W≡C^{t}Bu(THF)$_2$ (**8**) via treatment with MeOTf did not work. Instead, upon treatment with MeOTf in Et_2O/THF (4/1) the alkylidene complex **3** forms and signals tentatively assigned to the oxo-alkyl complex [CBZ-ONO]W≡O(CH_2^{t}Bu) (**6**) appear in the ^{1}H and ^{19}F NMR spectra (C_6D_6), according to Scheme 4. Four quartet resonances in the ^{19}F NMR spectrum, two quartets attributable to **3** and two quartets at −73.48 and −74.33 ppm to complex **6** (Figure S25 in the Supporting Information), confirm the presence of two distinct complexes in the reaction mixture. The tentative assignment for **6** in the reaction mixture is based on an *in situ* experiment between **3** and MeOTf (*vide infra*). Complex **3** presumably forms from adventitious protons, a fact verified by the addition of HCl in diethyl ether to **4**. Complex **6** likely originates from alkylidene **3**, generated *in situ* and MeOTf through isobutylene expulsion. Isobutylene expulsion is common for these complexes and was reported previously for the flexible alkylidene.[23] Treating the alkylidene **3** directly with MeOTf provides the oxo-alkyl complex **6** *in situ* along with isobutylene. Complex **6** exhibits methylene resonances for the neopentyl group at 3.08 ppm, and the corresponding ^{t}Bu protons resonate at 1.43 ppm in the ^{1}H NMR spectrum. The methyl protons on the pincer backbone appear at 2.19 ppm (Figure S28 in the Supporting Information). Two quartet

https://dx.doi.org/10.1021/acs.organomet.0c00150
Organometallics 2020, 39, 2207−2213

Scheme 4. Synthetic Attempt to Access the Neutral Alkylidyne [CBZ-ONO]W≡C^{t}Bu(THF)$_2$ (8) and Generation of Oxo-alkyl Complex [CBZ-ONO]W≡O(CH$_2$^{t}Bu) (6)

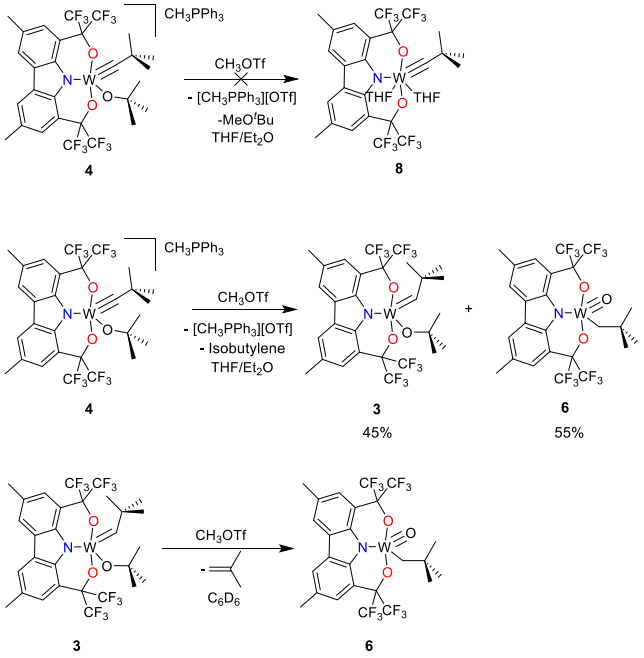

resonances, previously observed in the reaction between **4** and MeOTf (*vide supra*), appear at −73.48 and −74.33 ppm in the ^{19}F NMR spectrum (Figure S31 in the Supporting Information). Attempts to trap any neutral alkylidyne generated *in situ* with 1-phenyl-1-propyne to form a metallacyclobutadiene also failed.

Density functional theory (DFT) calculations were performed to examine the electronic structure of the complexes and to compare the flexible versus rigid ligand composition on the orbital overlap in the inorganic enamine. Geometry optimization and frequency calculations for alkylidene **3** were performed using spin-restricted DFT employing the hybrid functional B3LYP[38,39]/SDD[40]/triple-ζ TZVP[41] basis sets from the Gaussian 09 program suite.[42] Molecular orbitals were generated using Gabedit[43] at the specified isovalues (0.05).

To calibrate, atomic coordinates from the crystal structure of alkylidene complex **3** serve as the input for geometry optimization. Figure 5 and Table 1 exhibit the bond lengths and bond angles of the computed structure **3′** and of **3**. The structural parameters of **3′** are in good agreement the experimental metrics for **3**. For example, the sum of the angles around the pincer N1 atom in **3′** adds up to 359.8°, matching well with the experimental value of 360.0(3)°. Also, somewhat longer, but reasonable, the calculation estimates correctly the W1═C25 alkylidene bond (1.879(5)$_{ex}$/1.903$_{cal}$ Å) and the N1−W1 bond of the pincer (2.013(4)$_{ex}$/2.050$_{cal}$ Å). The ligand being rigid, the calculation does not show any twist in the backbone, as expected.

Geometry optimization and frequency calculations were also performed for the anionic alkylidyne complex anions {[CBZ-ONO]W≡C^{t}Bu(O^{t}Bu)}$^-$ (**4**) and {[CF$_3$-ONO]W≡C^{t}Bu-(O^{t}Bu)}$^-$ (**7**)[32] using hybrid functional B3LYP/triple-ζ Def2TZVP[41,44] level theory. Table S2 in the Supporting Information gives the metric parameters for computed

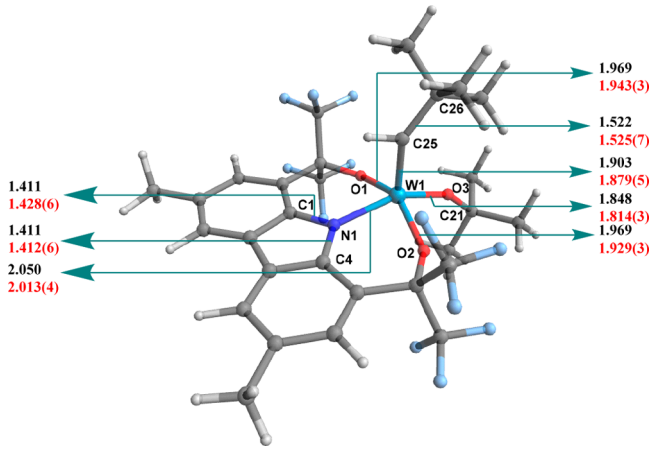

Figure 5. Geometry-optimized structure of **3′** using B3LYP/SDD/triple-ζ TZVP level theory and comparison to the experimental values obtained for complex **3**.

Table 1. Selected Bond Lengths (Å) and Angles (deg) for the Single-Crystal X-ray Structure of 3 and DFT Geometry-Optimized Structure of 3′

	3	3′ (B3LYP/SDD/TZVP)
	Bond Lengths (Å)	
W1═C25	1.879(5)	1.903
C25−C26	1.525(7)	1.522
W1−O2	1.929(3)	1.969
W1−O1	1.943(3)	1.969
W1−O3	1.814(3)	1.848
W1−N1	2.013(4)	2.050
N1−C4	1.412(6)	1.411
N1−C1	1.428(6)	1.411
	Bond Angles (deg)	
∠W1═C25−C26	139.1(4)	139.6
∠W1−O3−C21	143.8(3)	152.8
∠N1−W1−O3	146.4(16)	151.4
∠O1−W1−O2	149.9(15)	147.1
∠C4−N1−C1	105.7(4)	106.4
∠C4−N1−W1	127.5(3)	126.7
∠C1−N1−W1	126.8(3)	126.7
∠O1−W1−N1	81.75(15)	81.08

structures **4′** and **7′**. The structural parameters of **4′** are in good agreement with the parameters of **7′**. For example, the W1−N1 bond length for **4′** (2.165 Å) compares well with the W1−N1 bond length for **7′** (2.161 Å). Similarly, the W1≡C25 alkylidyne bond lengths (1.759 Å for **4′** and 1.765 Å for **7′**), the C25−C26 bond lengths (1.490 Å for **4′** and 1.493 Å for **7′**), the W1−O2 bond lengths (1.980 Å for **4′** and 1.982 Å for **7′**), and the W1−O1 bond lengths (1.983 Å for **4′** and 1.989 Å for **7′**) are also in good agreement. Consistent with the bond lengths, the bond angle values are also similar for **4′** and **7′**. For example, the ∠W1≡C25−C26 bond angles (177.7° for **4′** and 176.6° for **7′**) and the ∠N1−W1≡C25 bond angles (98.60° for **4′** and 101.0° for **7′**) are in good agreement. Figure 6 depicts a comparison of the inorganic enamine bonding interaction between the computed structures **4′** and **7′**. Overall, the HOMO for **4′** is lower by approximately 0.245 eV (0.009 au) in comparison to **7′**. This computed result reflects the experimental UV−vis data, where complex **4** exhibits a λ_{max} value at 389.4 nm (ε = 3254(84) m^2/mol) and

https://dx.doi.org/10.1021/acs.organomet.0c00150
Organometallics 2020, 39, 2207−2213

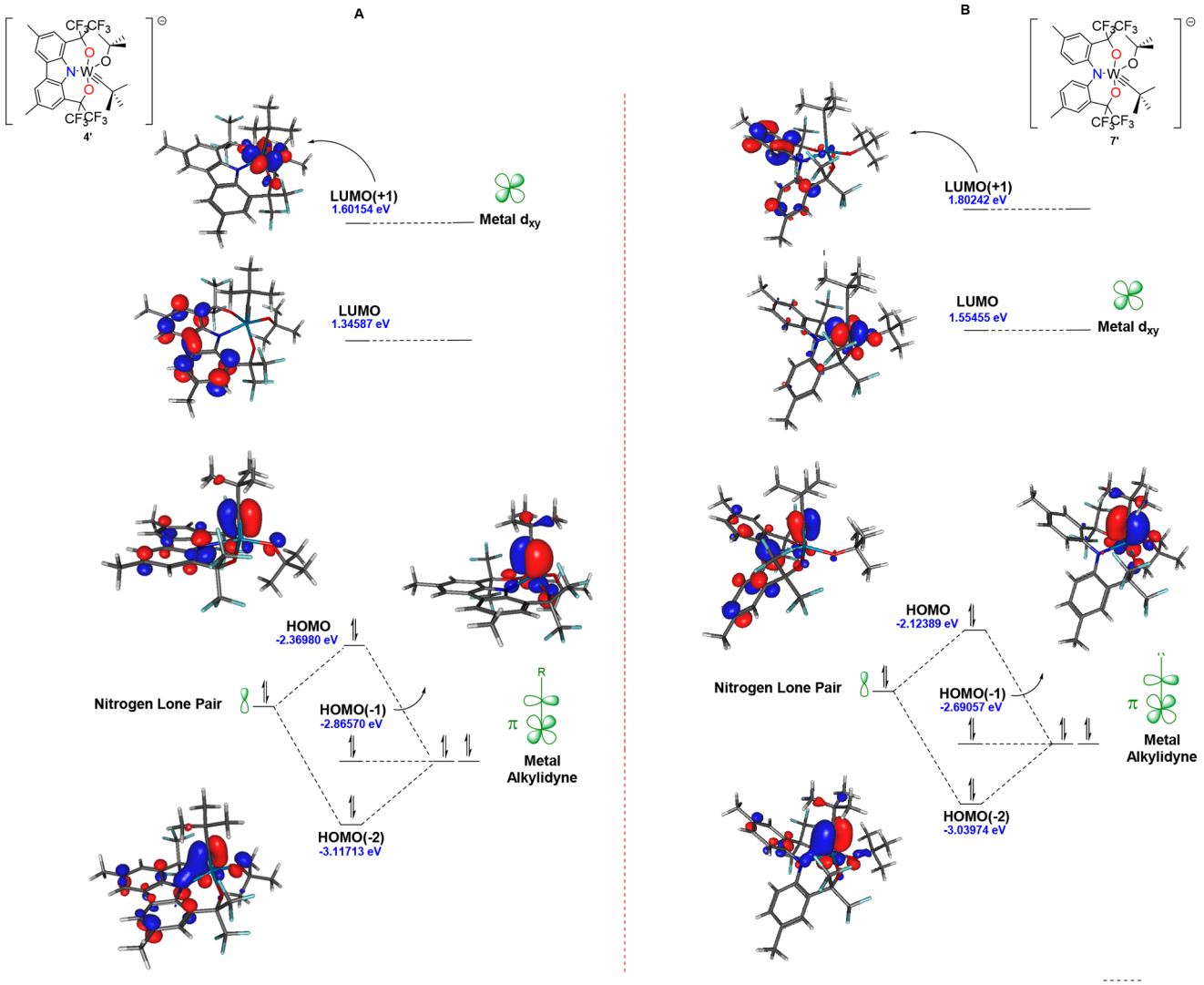

Figure 6. Truncated molecular orbital diagrams (B3LYP/Def2TZVP) exhibiting inorganic enamine bonding combinations for the anions {[CBZ-ONO]W≡C^{t}Bu(O^{t}Bu)}$^-$ (**4′**) (left) and {[CF_3-ONO]W≡C^{t}Bu(O^{t}Bu)}$^-$ (**7′**) (right).

complex **7** is red-shifted to 478.3 nm (ε = 648(91) m^2/mol). It is evident from the computed structures that the nitrogen atom lone pair is nearly collinear with the alkylidyne π orbitals in both complexes. As a consequence, the bonding interaction generates an inorganic enamine between the HOMO(-2) and the HOMO. The magnitude of the interaction as judged by the difference in energy between the HOMO(-2) and the HOMO is slightly lower for the rigid [CBZ-ONO]$^{3-}$ ligand (0.747 eV or 0.027 au) than for the flexible [CF_3-ONO]$^{3-}$ ligand (0.915 eV or 0.033 au). Designed to examine the effect of p orbital orientation on the magnitude of the inorganic enamine effect, the rigid ligand was expected to have a significantly stronger overlap. However, several factors other than p orbital orientation must influence the magnitude of the overlap. For example, there is a distinct difference in the magnitudes of the electron density on the N atom within the molecular orbitals that overlap with the W−C π bond for **4′** and **7′**.

In **4′** the electron density is spread out within the carbazole framework, whereas in the twisted ligand, it is largely centered on the N atom, thus greatly enhancing the overlap. An implication that this feature is not the same in both cases is that in **4′** the LUMO is a carbazole ligand-centered molecular orbital, whereas in **7′** it is the d_{xy} orbital that contains some π* character. In **4′**, the d_{xy} orbital is the LUMO(+1). The ligand-centered LUMO for **4′** is an obvious consequence of lowered π* orbitals from delocalization in the planar carbazole ring system.

To summarize this work, the new rigid trianionic carbazole based pincer proligand [CBZ-ONO]H_3 (**2**) was synthesized. Using the new ligand, tungsten alkylidene (**3**) and anionic alkylidyne (**4**) complexes were synthesized and characterized. A comparison of the solid-state structures between rigid **3** and flexible **5** alkylidene complexes reveals dramatic structural differences. Perhaps due to the structural differences, in particular the rigidity imparted by the carbazole ligand, the neutral alkylidyne complex could not be synthesized. Instead, consistent with previously observed reactivity, evidence for the generation of the oxo-alkyl complex **6** and isobutylene expulsion comes from NMR spectroscopy. DFT calculations reveal inorganic enamine bonding for anionic alkylidyne complexes of both ligands, though the magnitude of the overlap is similar for both. Achieving the objective, the original motivation for this work was to maximize the inorganic enamine effect by restricting the p orbital on the N atom of the pincer to be perfectly collinear with the W−C π bond. In hindsight, obvious factors are at play in maximizing the

https://dx.doi.org/10.1021/acs.organomet.0c00150
Organometallics 2020, 39, 2207−2213

magnitude of the overlap, such as the N atom p orbital electron density in the wave function involved in overlapping with the W−C π bond and their relative energies. Nonetheless, the flexible $[CF_3\text{-}ONO]^{3-}$ and new rigid $[CBZ\text{-}ONO]^{3-}$ are useful ligand partners that allow for the direct interrogation of ligand flexibility on structure and reactivity in transition-metal complexes or catalysts.

Caution! Hexafluoroacetone is a highly volatile and toxic gas and must be used in a well-ventilated fume hood.

■ ASSOCIATED CONTENT

Supporting Information

The Supporting Information is available free of charge at https://pubs.acs.org/doi/10.1021/acs.organomet.0c00150.

Full experimental details, including NMR data and spectra for new compounds, and X-ray crystal structure data (PDF)

Cartesian coordinates for the calculated structures (XYZ)

Accession Codes

CCDC 1973154 contains the supplementary crystallographic data for this paper. These data can be obtained free of charge via www.ccdc.cam.ac.uk/data_request/cif, or by emailing data_request@ccdc.cam.ac.uk, or by contacting The Cambridge Crystallographic Data Centre, 12 Union Road, Cambridge CB2 1EZ, UK; fax: +44 1223 336033.

■ AUTHOR INFORMATION

Corresponding Author

Adam S. Veige − *University of Florida, Department of Chemistry, Center for Catalysis, Gainesville, Florida 32611, United States;* orcid.org/0000-0002-7020-9251; Email: veige@chem.ufl.edu

Authors

Ushnish Mandal − *University of Florida, Department of Chemistry, Center for Catalysis, Gainesville, Florida 32611, United States*

Sudarsan VenkatRamani − *University of Florida, Department of Chemistry, Center for Catalysis, Gainesville, Florida 32611, United States;* orcid.org/0000-0003-2836-0705

Ion Ghiviriga − *University of Florida, Department of Chemistry, Center for Catalysis, Gainesville, Florida 32611, United States*

Khalil A. Abboud − *University of Florida, Department of Chemistry, Center for Catalysis, Gainesville, Florida 32611, United States*

Complete contact information is available at: https://pubs.acs.org/10.1021/acs.organomet.0c00150

Notes

The authors declare no competing financial interest.

■ ACKNOWLEDGMENTS

A.S.V. acknowledges the NSF (CHE-1856674) for providing funding for this research. K.A.A. acknowledges the NSF (CHE-0821346) for the purchase of X-ray equipment.

■ REFERENCES

(1) Peris, E.; Crabtree, R. H. Key factors in pincer ligand design. *Chem. Soc. Rev.* **2018**, *47*, 1959−1968.

(2) Lawrence, M. A. W.; Green, K. A.; Nelson, P. N.; Lorraine, S. C. Review: Pincer ligands-tunable, versatile and applicable. *Polyhedron* **2018**, *143*, 11−27.

(3) Elser, I.; Groos, J.; Hauser, P. M.; Koy, M.; van der Ende, M.; Wang, D. R.; Frey, W.; Wurst, K.; Meisner, J.; Ziegler, F.; Kastner, J.; Buchmeiser, M. R. Molybdenum and tungsten alkylidyne complexes containing mono-, bi-, and tridentate N-heterocyclic carbenes. *Organometallics* **2019**, *38*, 4133−4146.

(4) Begum, R. A.; Powell, D.; Bowman-James, K. Thioamide pincer ligands with charge versatility. *Inorg. Chem.* **2006**, *45*, 964−966.

(5) van Leeuwen, P.; Kamer, P. C. J.; Reek, J. N. H. The bite angle makes the catalyst. *Pure Appl. Chem.* **1999**, *71*, 1443−1452.

(6) Sugiyama, H.; Korobkov, I.; Gambarotta, S.; Moller, A.; Budzelaar, P. H. M. Preparation, characterization, and magnetic behavior of the ln derivatives (ln = Nd, La) of a 2,6-diiminepyridine ligand and corresponding dianion. *Inorg. Chem.* **2004**, *43*, 5771−5779.

(7) Lyaskovskyy, V.; de Bruin, B. Redox non-innocent ligands: Versatile new tools to control catalytic reactions. *ACS Catal.* **2012**, *2*, 270−279.

(8) de Miguel, Y. R. Supported catalysts and their applications in synthetic organic chemistry. *J. Chem. Soc. Perk. T 1* **2000**, 4213−4221.

(9) O'Reilly, M. E.; Veige, A. S. Trianionic pincer and pincer-type metal complexes and catalysts. *Chem. Soc. Rev.* **2014**, *43*, 6325−6369.

(10) O'Reilly, M.; Falkowski, J. M.; Ramachandran, V.; Pati, M.; Abboud, K. A.; Dalal, N. S.; Gray, T. G.; Veige, A. S. Catalytic aerobic oxidation by a trianionic pincer cr^{III}/cr^{V} couple. *Inorg. Chem.* **2009**, *48*, 10901−10903.

(11) Nguyen, A. I.; Zarkesh, R. A.; Lacy, D. C.; Thorson, M. K.; Heyduk, A. F. Catalytic nitrene transfer by a zirconium(IV) redox-active ligand complex. *Chem. Sci.* **2011**, *2*, 166−169.

(12) Heyduk, A. F.; Zarkesh, R. A.; Nguyen, A. I. Designing catalysts for nitrene transfer using early transition metals and redox-active ligands. *Inorg. Chem.* **2011**, *50*, 9849−9863.

(13) Zarkesh, R. A.; Heyduk, A. F. Reactivity of diazoalkanes with tantalum(V) complexes of a tridentate amido-bis(phenolate) ligand. *Organometallics* **2009**, *28*, 6629−6631.

(14) McGowan, K. P.; Veige, A. S. A neutral trianionic pincer ncn Cr^{IV}-Me complex as a highly active ethylene polymerization precatalyst. *J. Organomet. Chem.* **2012**, *711*, 10−14.

(15) Sarkar, S.; McGowan, K. P.; Kuppuswamy, S.; Ghiviriga, I.; Abboud, K. A.; Veige, A. S. An oco^{3-} trianionic pincer tungsten(VI) alkylidyne: Rational design of a highly active alkyne polymerization catalyst. *J. Am. Chem. Soc.* **2012**, *134*, 4509−4512.

(16) McGowan, K. P.; O'Reilly, M. E.; Ghiviriga, I.; Abboud, K. A.; Veige, A. S. Compelling mechanistic data and identification of the active species in tungsten-catalyzed alkyne polymerizations: Conversion of a trianionic pincer into a new tetraanionic pincer-type ligand. *Chem. Sci.* **2013**, *4*, 1145−1155.

(17) Gonsales, S. A.; Kubo, T.; Flint, M. K.; Abboud, K. A.; Sumerlin, B. S.; Veige, A. S. Highly tactic cyclic polynorbornene: Stereoselective ring expansion metathesis polymerization of norbornene catalyzed by a new tethered tungsten-alkylidene catalyst. *J. Am. Chem. Soc.* **2016**, *138*, 4996−4999.

(18) Nadif, S. S.; Kubo, T.; Gonsales, S. A.; VenkatRamani, S.; Ghiviriga, I.; Sumerlin, B. S.; Veige, A. S. Introducing "ynene" metathesis: Ring-expansion metathesis polymerization leads to highly cis and syndiotactic cyclic polymers of norbornene. *J. Am. Chem. Soc.* **2016**, *138*, 6408−6411.

(19) Roland, C. D.; Li, H.; Abboud, K. A.; Wagener, K. B.; Veige, A. S. Cyclic polymers from alkynes. *Nat. Chem.* **2016**, *8*, 791−796.

(20) Niu, W. J.; Gonsales, S. A.; Kubo, T.; Bentz, K. C.; Pal, D.; Savin, D. A.; Sumerlin, B. S.; Veige, A. S. Polypropylene: Now available without chain ends. *Chem.* **2019**, *5*, 237−244.

(21) Miao, Z. H.; Kubo, T.; Pal, D.; Sumerlin, B. S.; Veige, A. S. Ph-responsive water-soluble cyclic polymer. *Macromolecules* **2019**, *52*, 6260−6265.

(22) McGowan, K. P.; Abboud, K. A.; Veige, A. S. Trianionic NCN^{3-} pincer complexes of chromium in four oxidation states (Cr^{II}, Cr^{III},

Cr^{IV}, Cr^{V}): Determination of the active catalyst in selective 1-alkene to 2-alkene isomerization. *Organometallics* **2011**, *30*, 4949−4957.
(23) O'Reilly, M. E.; Ghiviriga, I.; Abboud, K. A.; Veige, A. S. A new ONO^{3-} trianionic pincer-type ligand for generating highly nucleophilic metal-carbon multiple bonds. *J. Am. Chem. Soc.* **2012**, *134*, 11185−11195.
(24) Gonsales, S. A.; Pascualini, M. E.; Ghiviriga, I.; Abboud, K. A.; Veige, A. S. Fast ″Wittig-like″ reactions as a consequence of the inorganic enamine effect. *J. Am. Chem. Soc.* **2015**, *137*, 4840−4845.
(25) Gonsales, S. A.; Pascualini, M. E.; Ghiviriga, I.; Veige, A. S. Evidence for a zwitterionic transition state double bond rotations within tungsten-vinyl complexes. *Chem. Commun.* **2015**, *51*, 13404−13407.
(26) Gonsales, S. A.; Ghiviriga, I.; Abboud, K. A.; Veige, A. S. Carbon dioxide cleavage across a tungsten-alkylidyne bearing a trianionic pincer-type ligand. *Dalton Trans.* **2016**, *45*, 15783−15785.
(27) VenkatRamani, S.; Huff, N. B.; Jan, M. T.; Ghiviriga, I.; Abboud, K. A.; Veige, A. S. New alkylidyne complexes featuring a flexible trianionic ONO^{3-} pincer-type ligand: Inorganic enamine effect versus sterics in electrophilic additions. *Organometallics* **2015**, *34*, 2841−2848.
(28) Lu, Z. K.; Gao, Y.; Chen, H.; Liu, Z.; Sun, L. C. Water oxidation catalyzed by a charge-neutral mononuclear ruthenium(III) complex. *Dalton Trans.* **2017**, *46*, 1304−1310.
(29) Britovsek, G. J. P.; Gibson, V. C.; Hoarau, O. D.; Spitzmesser, S. K.; White, A. J. P.; Williams, D. J. Iron and cobalt ethylene polymerization catalysts: Variations on the central donor. *Inorg. Chem.* **2003**, *42*, 3454−3465.
(30) Listemann, M. L.; Schrock, R. R. Multiple metal-carbon bonds. 35. A general route to tri-tert-butoxytungsten alkylidyne complexes. Scission of acetyleenes by ditungsten hexa-tert-butoxide. *Organometallics* **1985**, *4*, 74−83.
(31) Addison, A. W.; Rao, T. N.; Reedijk, J.; Vanrijn, J.; Verschoor, G. C. Synthesis, structure, and spectroscopic properties of copper(II) compounds containing nitrogen sulfur donor ligands: The crystal and molecular structure of aqua 1,7-bis-(N-methylbenzimidazol-2′-yl)-2,6-dithiaheptane copper(II) perchlorate. *J. Chem. Soc., Dalton Trans.* **1984**, 1349−1356.
(32) O'Reilly, M. E.; Ghiviriga, I.; Abboud, K. A.; Veige, A. S. Unusually stable tungstenacyclobutadienes featuring an ono trianionic pincer-type ligand. *Dalton Trans.* **2013**, *42*, 3326−3336.
(33) Bestmann, H. J.; Stransky, W.; Vostrowsky, O. Reactions of alkylidnetriphenylphosphorane, XXXIII. Preparation of lithium salt free ylide solutions with sodium bis(trimethylsilyl)amide as base. *Chem. Ber.* **1976**, *109*, 1694−1700.
(34) Tonzetich, Z. J.; Schrock, R. R.; Muller, P. Reaction of phosphoranes with $Mo(N\text{-}2,6\text{-}i\text{-}Pr_2C_6H_3)(CHCMe_3)[OCMe(CF_3)_2]_2$: Synthesis and reactivity of an anionic imido alkylidyne complex. *Organometallics* **2006**, *25*, 4301−4306.
(35) VenkatRamani, S.; Ghiviriga, I.; Abboud, K. A.; Veige, A. S. A new ONO^{3-} trianionic pincer ligand with intermediate flexibility and its tungsten alkylidene and alkylidyne complexes. *Dalton Trans.* **2015**, *44*, 18475−18486.
(36) O'Reilly, M. E.; Nadif, S. S.; Ghiviriga, I.; Abboud, K. A.; Veige, A. S. Synthesis and characterization of tungsten alkylidene and alkylidyne complexes supported by a new pyrrolide-centered trianionic ONO^{3-} pincer-type ligand. *Organometallics* **2014**, *33*, 836−839.
(37) Nadif, S. S.; O'Reilly, M. E.; Ghiviriga, I.; Abboud, K. A.; Veige, A. S. Remote multiproton storage within a pyrrolide-pincer-type ligand. *Angew. Chem., Int. Ed.* **2015**, *54*, 15138−15142.
(38) Becke, A. D. Density-functional thermochemistry 0.3. The role of exact exchange. *J. Chem. Phys.* **1993**, *98*, 5648−5652.
(39) Lee, C. T.; Yang, W. T.; Parr, R. G. Development of the colle-salvetti correlation-energy formula into a functional of the electron-density. *Phys. Rev. B: Condens. Matter Mater. Phys.* **1988**, *37*, 785−789.
(40) Dunning, J. T. H.; Hay, P. J. In *Modern Theoretical Chemistry*; Plenum: New York, 1976; pp 1−28.
(41) Weigend, F.; Ahlrichs, R. Balanced basis sets of split valence, triple zeta valence and quadruple zeta valence quality for h to rn: Design and assessment of accuracy. *Phys. Chem. Chem. Phys.* **2005**, *7*, 3297−3305.
(42) Frisch, M. J.; Trucks, G. W.; Schlegel, H. B.; Scuseria, G. E.; Robb, M. A.; Cheeseman, J. R.; Scalmani, G.; Barone, V.; Petersson, G. A.; Nakatsuji, H.; Li, X.; Caricato, M.; Marenich, A.; Bloino, J.; Janesko, B. G.; Gomperts, R.; Mennucci, B.; Hratchian, H. P.; Ortiz, J. V.; Izmaylov, A. F.; Sonnenberg, J. L.; WilliamsYoung, D.; Ding, F.; Lipparini, F.; Egidi, F.; Goings, J.; Peng, B.; Petrone, A.; Henderson, T.; Ranasinghe, D.; Zakrzewski, V. G.; Gao, J.; Rega, N.; Zheng, G.; Liang, W.; Hada, M.; Ehara, M.; Toyota, K.; Fukuda, R.; Hasegawa, J.; Ishida, M.; Nakajima, T.; Honda, Y.; Kitao, O.; Nakai, H.; Vreven, T.; Throssell, K.; Montgomery, J. A., Jr.; Peralta, J. E.; Ogliaro, F.; Bearpark, M.; Heyd, J. J.; Brothers, E.; Kudin, K. N.; Staroverov, V. N.; Keith, T.; Kobayashi, R.; Normand, J.; Raghavachari, K.; Rendell, A.; Burant, J. C.; Iyengar, S. S.; Tomasi, J.; Cossi, M.; Millam, J. M.; Klene, M.; Adamo, C.; Cammi, R.; Ochterski, J. W.; Martin, R. L.; Morokuma, K.; Farkas, O.; Foresman, J. B.; Fox, D. J. *Gaussian 09, rev. d.01*; Gaussian, Inc.: Wallingford, CT, 2016.
(43) Allouche, A. R. Gabedit-a graphical user interface for computational chemistry softwares. *J. Comput. Chem.* **2011**, *32*, 174−182.
(44) Weigend, F. Accurate coulomb-fitting basis sets for h to rn. *Phys. Chem. Chem. Phys.* **2006**, *8*, 1057−1065.

https://dx.doi.org/10.1021/acs.organomet.0c00150
Organometallics 2020, 39, 2207−2213